Detection and capture of breast cancer cells with photoacoustic flow cytometry

Kiran Bhattacharyya
Benjamin S. Goldschmidt
John A. Viator

Detection and capture of breast cancer cells with photoacoustic flow cytometry

Kiran Bhattacharyya,[a] Benjamin S. Goldschmidt,[b] and John A. Viator[b,*]
[a]Northwestern University, Department of Biomedical Engineering, 2145 Sheridan Road, Evanston, Illinois 60208, United States
[b]Duquesne University, Biomedical Engineering Program, 309 Libermann Hall, Pittsburgh, Pennsylvania 15282, United States

Abstract. According to the Centers for Disease Control and Prevention, breast cancer is the most common cancer and the second leading cause of cancer related deaths among women. Metastasis—the presence of secondary tumors caused by the spread of cancer cells via the circulatory or lymphatic systems—significantly worsens the prognosis of any breast cancer patient. A technique is developed to detect circulating breast cancer cells in human blood using a photoacoustic flow cytometry method. A Q-switched laser is used to interrogate thousands of blood cells with one pulse as they flow through the beam path. Cells that are optically absorbing, either naturally or artificially, emit an ultrasound wave as a result of the photoacoustic (PA) effect. Breast cancer cells are targeted with chromophores through immunochemistry in order to enhance optical absorption. After which, the PA cytometry device is calibrated to demonstrate the ability to detect single cells. Cultured breast cancer cells are added to whole blood to reach a biologically relevant concentration of about 25 to 45 breast cancer cells per 1 mL of blood. An *in vitro* PA flow cytometer is used to detect and isolate these cells followed by capture with the use of a micromanipulator. This method can not only be used to determine the disease state of the patient and the response to therapy but also it can be used for genetic testing and *in vitro* drug trials since the circulating cell can be captured and studied. © *The Authors. Published by SPIE under a Creative Commons Attribution 3.0 Unported License. Distribution or reproduction of this work in whole or in part requires full attribution of the original publication, including its DOI.* [DOI: 10.1117/1.JBO.21.8.087007]

1 Introduction

The spread of cancer from the primary tumor to distant organs is caused by the invasion of cancer cells into the vasculature or lymphatic system. This is followed by eventual deposition and growth in a preferred location in tissue.[1] Research has indicated that the concentration of these circulating tumor cells (CTCs) is a significant prognostic factor.[2–4] The biologically relevant concentration of these CTCs (0 to 1000 cells/mL of blood) is much smaller than the number of erythrocytes (10^9 to 10^{10} cells/mL) and leukocytes (10^6 to 10^7 cells/mL) in blood, complicating the task of detection.[5]

Photoacoustic flow cytometry (PAFC) has been used both *in vivo* and *in vitro* to detect circulating melanoma cells, which are naturally optically absorbing.[6,7] Most other cancers are nonpigmented and inaccessible to PAFC without cellular alteration. Viator et al.[8] demonstrated the ability to add gold nanoparticles (AuNPs) to prostate cancer cells through immunochemistry and detect them using the *in vitro* cytometry method. Magnetic particles have also been used for *in vivo* photoacoustic (PA) cytometry for both optical contrast and to aggregate CTCs for increased signal-to-noise ratio.[9] Additionally, nanoparticle attachment to melanoma cells has been considered in order to increase signal contrast and consistency, since melanin expression is susceptible to biological variability.[10–12] Finally, Bhattacharyya et al.[13] demonstrated attachment of antibody-conjugated AuNPs to breast cancer cells and consequent detection in saline with *in vitro* PAFC.

Significant research has been performed on *in vivo* PAFC[14] with applications of CTC detection in the mouse model. However, the method of translation to human studies remains unclear due to the larger blood volumes, increased light scattering due to deeper tissue positions of vasculature, and difficulty in validating false positives. On the other hand, CTCs detected with *in vitro* PAFC can be validated to be cancer cells and captured for further testing. O'Brien et al.[15] demonstrated the ability to capture circulating melanoma cells with *in vitro* two-phase PAFC. This technique of *in vitro* two-phase PAFC was also used by Gupta et al.[16] to detect and capture circulating melanoma cells in an induced mouse melanoma model. In two-phase PAFC, the aqueous cell suspension to be tested is flowed into the flow chamber along with air. When the two immiscible fluids are flowed simultaneously into the same chamber, they form alternating compartments or slugs of each fluid, referred to as the two phases.[17]

However, oil, in place of air, can also be used for the two-phase PAFC since oil still does not mix with aqueous cell solutions, which are mostly water. In this study, two-phase PAFC with oil and nanoparticle enrichment of cancer cells are combined to create the complete *in vitro* CTC detection and capture system. Feature extraction from emitted PA signals and classification algorithms are used for the automated detection of cancer cells. Healthy blood is spiked with breast cancer cells, tested with the PAFC, and detected cells are isolated. Finally, a micromanipulator is used to extract single CTCs.

*Address all correspondence to: John A. Viator, E-mail: viatorj@duq.edu

2 Material and Methods

2.1 Antibody-Nanoparticle Conjugation

First, 45 μL of streptavidin coated 320 nm red flourescent latex nanoparticles (Bangs Laboratories, Fishers, Indiana) were added to 1.5 μL of biotin conjugated anti-EpCAM monoclonal antibody (Pierce Antibodies, Rockford, Illinois) in 500 μL of 1× PBS. This suspension was incubated at 22°C for 1 h. Then, 20 μL of neutravidin-conjugated 54-nm spherical AuNPs was added to the suspension with an additional 500 μL of 1× PBS and allowed to incubate for 20 min. Finally, 1.5 μL of anti-EpCAM in another 500 μL of 1× PBS was added to the suspension and allowed to incubate for 30 min. The resulting suspension was centrifuged at 550 × g for 8 min in order to pellet the nanoparticles and leave the excess antibodies in suspension. The supernatant was removed and the nanoparticle pellet was resuspended in 1 mL of 1× PBS.

2.2 Blood Centrifugation Procedure

In a 15-mL conical cuvette, 1 mL of blood drawn from a healthy individual was layered onto 3 mL of Histopaque 1077 (Sigma Aldrich, St. Louis, Missouri), which is widely used to separate leukocytes from erythrocytes, and centrifuged at 400 × g for 30 min. After centrifugation, the peripheral mononuclear blood cell (PBMC) layer was withdrawn with a transfer pipette and placed in another conical cuvette. The cancer cells in blood are expected to be in the PBMC layer due to their similarity in density with mononuclear leukocytes. This was diluted with 10 mL of 1× PBS and centrifuged at 300 × g for 15 min. The supernatant was removed and the cell pellet was resuspended in 500 μL of 1× PBS and 500 μL of red blood cell lysis solution (G-Biosciences St. Louis, Missouri). This solution was agitated every 2 to 3 min for 10 min to aid in lysing the remaining erythrocytes, which may cause false-positive signals due to hemoglobin pigment. After 10 min, this solution was diluted in 2 mL of 1× PBS and centrifuged at 140 × g for 10 min. The supernatant was removed and the cell pellet was resuspended in 1 mL of 1× PBS.

2.3 Nanoparticle Attachment to Breast Cancer Cells

The following protocols were developed to investigate if the nanoparticles were just attaching to the EpCAM surface receptors exclusively on breast cancer cells or unknown targets, which were not specific to the anti-EpCAM antibody. Additionally, confocal imaging was used to determine if nanoparticles were internalized by the cells.

2.3.1 Specific labeling to EpCAM surface receptor

Cultured T47D breast cancer cells were diluted into a concentration of 10^5 cells/mL in 1 mL of 1× PBS and incubated with 4 μL of biotin conjugated anti-EpCAM monoclonal antibody for 1 h. An excess of anti-EpCAM antibody was used to ensure that all EpCAM receptors on the cells were blocked. Then, the cell suspension was centrifuged at 140 × g for 10 min in order to remove the excess unbound antibodies. The supernatant was removed and the breast cancer cell pellet was resuspended in 1 mL of 1× PBS and 40 μL of the fluorescent-AuNP suspension was added to the cell suspension. This solution was allowed to incubate for 1 h and then centrifuged at 140 × g for 10 min to

remove excess nanoparticles. The cell pellet was resuspended in 1 mL of 1× PBS.

The cells were then imaged with a Zeiss LSM 510 META NLO confocal microscope. A tetramethylrhodamine (TRITC) filter and excitation scheme was used to image the flourescent-gold particles attached to the breast cancer cells. A three-dimensional (3-D) z-stack was acquired from multiple cells with 1-μm step size with variable depths depending on the geometry of the cells.

2.3.2 Affinity to breast cancer cells in the presence of leukocytes

Cultured T47D breast cancer cells were diluted into a concentration of 10^5 cells/mL in 1 mL of 1× PBS and incubated with 10 μg/mL of 4',6-diamidino-2-phenylindole (DAPI) for 10 min in order to label the cancer cell nuclei for easy identification. Then the cell suspension was centrifuged at 140 × g for 10 min in order to remove the excess DAPI. The supernatant was removed and the breast cancer cell pellet was resuspended in the resulting leukocyte suspension from Sec. 2.2. After which, 40 μL of the fluorescent-AuNP suspension was added to the previously mentioned cell suspension. This solution was allowed to incubate for 1 h and then centrifuged at 140 × g for 10 min to remove excess nanoparticles. The cell pellet was resuspended in 1 mL of 1× PBS.

This suspension was then prepared on a slide and imaged with an Olympus IX-70 microscope with wide-field fluorescent capability and a 20× air objective. For the DAPI nuclear stain and the red-fluorescent AuNPs, the DAPI and TRITC filters were used, respectively. An exposure of 5 ms was used to capture the DAPI fluorescence, while a 100 ms exposure was required to capture the fluorescence from the fluorescent AuNP.

2.3.3 Intracellular distribution of nanoparticle labeling

Cultured T47D breast cancer cells were diluted into a concentration of 10^5 cells/mL in 1 mL of 1× PBS and incubated with 40 μL of the fluorescent-AuNP suspension. This solution was allowed to incubate for 1 h and then centrifuged at 140 × g for 10 min to remove excess nanoparticles. The cell pellet was resuspended in 1 mL of 1× PBS.

The cells were then imaged with a Zeiss LSM 510 META NLO confocal microscope. A TRITC filter and excitation scheme was used to image the flourescent-gold particles attached to the breast cancer cells. A 3-D z-stack was acquired from multiple cells with 1-μm step size with variable depths depending on the geometry of the cells.

2.4 Photoacoustic Flow Cytometry Detection

The *in vitro* two-phase PAFC system is composed of two programmable syringe pumps (Braintree Scientific, Braintree, Massachusetts), one with optical grade mineral oil (Fisher Scientific) and the other with the prepared cell sample to be tested. Both fluids were pumped at 20 μL/min simultaneously into a 1.5-mm diameter, 10-μm wall-thickness quartz flow chamber, creating alternating droplets of cell sample and oil, each ~7 μL in volume. A 1-mm optical fiber delivered 5 ns, 532 nm pulsed light transversely to a portion of the chamber (Fig. 1). The laser irradiated 3 μL of fluid with every pulse and the radiant exposure at the chamber was ~125 mJ/cm². An acoustic transducer with a 20-MHz bandwidth (Olympus,
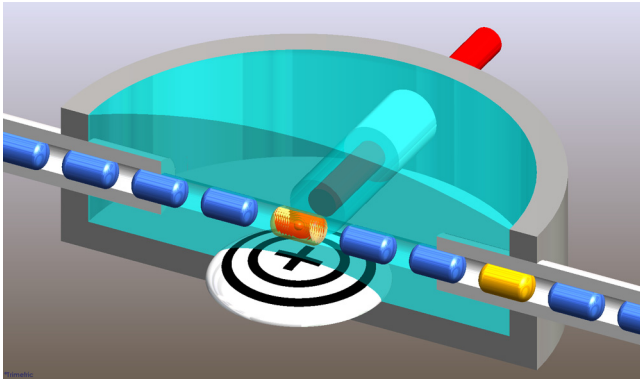
Fig. 1 An optical fiber, shown in red, irradiates droplets as they flow through the chamber. Droplets positive for cancer cells (yellow) produce light-induced ultrasound, which is detected by the acoustic transducer, shown as the target.

Waltham, Massachusetts) was coupled with the irradiated portion of the flow chamber to capture the PA emission. The analog signal was amplified 50 dB (Ritec Inc., Warwick, Rhode Island) and digitized with a LabVIEW integrated PXI card (National Instruments, Austin, Texas). The time resolution was 1 ns and the voltage resolution was 400 μV.

2.4.1 *Preliminary tests*

Breast cancer cells were tagged with nanoparticles using the same parameters as defined in Sec. 2.3 but not in the presence of leukocytes, so as to eliminate any false positives from nonspecific attachment. Then they were diluted into a concentration of ~670 cells/mL in 1 mL of 1× PBS. For this concentration of cells, approximately two cells are expected to be irradiated with each laser pulse, since 3 μL is the irradiated volume. This suspension was tested with the PAFC under the flow parameters previously described.

2.4.2 *Detection from centrifuged blood*

About 2 mL of blood from a donor was separated into two vials with 1 mL each. About 35 cancer cells with DAPI labeled nuclei and tagged with nanoparticles were added to one vial. Both vials of blood were centrifuged according to the procedure described in Sec. 2.2. The resulting solutions were tested with the PAFC detection system.

The vial without cancer cells was first run through the system. The PA signals from multiple droplets were used as a training set in order to determine the parameters of classification, following which, the vial with cancer cells was tested under the same parameters. The droplets that tested positive for cancer according to the classification algorithm were captured on a slide. Then a light microscope was used to visualize the cancer cells and withdraw them with a micromanipulator.

3 Results

3.1 *Nanoparticle Fabrication*

Large fluorescent spheres (300 nm) and smaller gold spheres (50 nm) were conjugated with Streptavidin–Biotin binding through anti-EpCAM antibodies. Fluorescent AuNPs were imaged with a scanning electron microscope to ensure that the expected results were achieved with the conjugation chemistry. Figure 2 has images of the fluorescent AuNPs showing that

the protocol described in Sec. 2.1 was successful in attaching the gold nanospheres to the larger fluorescent latex particles. Figure 2(b) demonstrates that clusters of particles also formed, which were on the 1-μm scale.

3.2 *Nanoparticle Attachment to Cancer Cells*

Breast cancer cells with DAPI-labeled nuclei were tagged with fluorescent-gold in the presence of leukocytes. Figure 3(b) demonstrates the high specificity of the fluorescent AuNP to the breast cancer cells, which are much larger than the surrounding leukocytes and platelets. However, there is some nonspecific attachment of the nanoparticles to the leukocytes, as shown by those that have been circled in yellow in Fig. 3(b). Approximately, 5% to 10% of leukocytes are nonspecifically labeled with nanoparticles. Those that are labeled have 6 to 10 times fewer nanoparticles on them compared to breast cancer cells, as can be determined through fluorescent intensity measurements based on pixel values (data not shown).

Nanoparticle attachment was both localized and diffuse in the breast cancer cell, as seen in Fig. 4. The dim red fluorescence from the entire cell is likely due to the single fluorescent-gold complexes, as shown in Fig. 2(a), whereas the brighter spots within the cell are from the clusters of nanoparticle complexes, as shown in Fig. 2(b).

Figure 5 compares labeling of a normal breast cancer cell with that of a cell that has EpCAM receptors blocked before exposure to the anti-EpCAM labeled nanoparticle complex. This verifies that the nanoparticle complex was attaching to the EpCAM receptors on the cancer cell.

3.3 *Photoacoustic Flow Cytometry Detection*

The PA signals captured with each irradiation was $x - y$ data with time and voltage values corresponding to acoustic pressure arriving at the ultrasound transducer at that moment. The chamber lasted 1 μs in time since it was 1.5 mm in diameter and the speed of sound in water is 1.5 mm/μs. Figure 6(a) shows a plot of the PA signal from within the chamber when there is just 1× PBS and Fig. 6(b) shows the PA signal from within the chamber when there are tagged breast cancer cells.

Two separate samples were tested with the PAFC system: 1× PBS and tagged breast cancer cells in 1× PBS at a concentration of 2 cells/3 μL. The PA waveform captured for each irradiation was saved and two features were extracted in postprocessing. One feature was the integral of the PA signal from within the flow chamber after every value was squared. This integral was adjusted by subtracting from it the squared-integral of a portion of the voltage trace outside the chamber, which was considered noise.

The second feature was a count within the chamber of the number of voltage values, which reached above a positive noise threshold or below a negative one. The noise thresholds were determined by a portion of the voltage trace outside the chamber as the 3σ boundaries of the noise, where σ denotes standard deviation. The count of values above or below the noise threshold was adjusted by subtracting from it the count from a portion of the voltage trace outside the chamber.

Figure 7 is a plot in feature space of each waveform collected from the two groups. There are 92 points in the control or 1× PBS group, while there are 64 points in the breast cancer cell group. The red boundary is an example of the 2.5σ boundary of the control group assuming the distribution is bivariate normal.
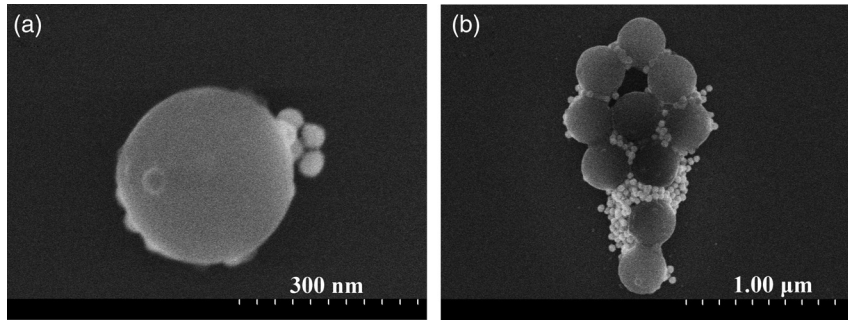
Fig. 2 Scanning electron microscope images of fluorescent AuNP. (a) Image of a single fluorescent sphere with multiple, smaller gold spheres attached. (b) Image of a cluster of fluorescent and gold spheres.
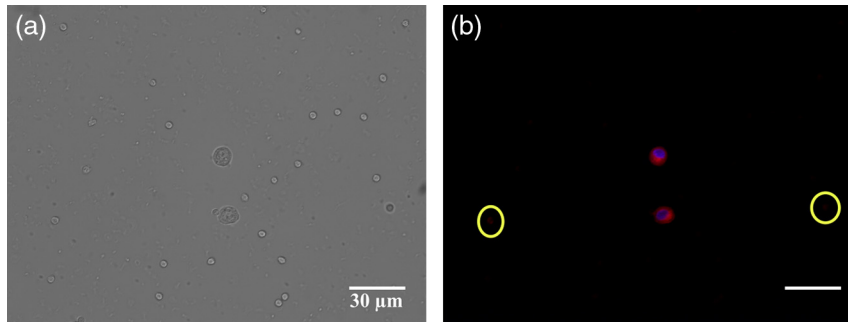

Fig. 3 Light microscope image of nanoparticle tagged breast cancer cells among leukocytes. (a) Transmitted light image of two T47D cells (largest, center) among numerous leukocytes (smaller, dispersed) and some platelets (smallest, irregular). (b) The corresponding fluorescent image showing highly fluorescent breast cancer cells (DAPI and NP fluorescence) with some nonspecifically labeled leukocytes circled in yellow.
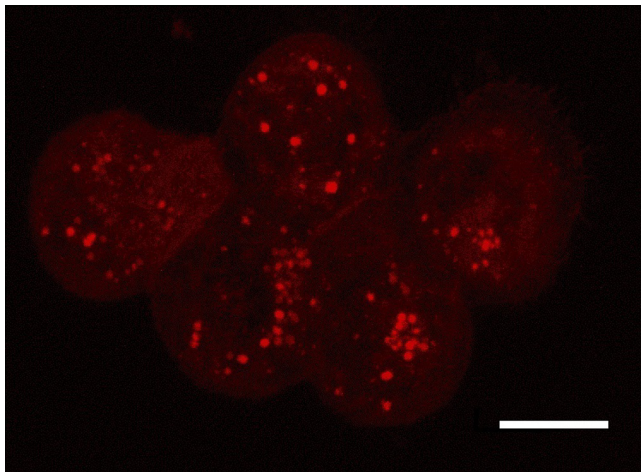

Fig. 4 Confocal microscope image of five nanoparticle tagged breast cancer cells to visualize localization and internalization of nanoparticles by cancer cells. The presence of nanoparticles, designated by red florescence, is both localized and diffuse as can be seen with the dim red hue and the bright red spots. The scale bar is 10 μm.

There is 1 control point outside the boundary and 43 out of 64 (67%) breast cancer cell points outside the boundary. This threshold can be used as a binary classifier and if the threshold is changed, then the true and false positive rates also change.

The boundaries of the 2.5σ threshold are calculated with Eq. (1). Starting with circle, R, centered around the origin

with a radius of 2.5 and transforming it into the ellipse, R' is seen in Fig. 7:

$$R' = \Phi \Lambda^{\frac{1}{2}} R, \tag{1}$$

where Λ are the eigenvalues of the covariance matrix of the $1\times$ PBS feature distribution and Φ are the eigenvectors. This is called unwhitening or coloring the standard bivariate normal distribution.

Figure 8 shows the receiver operating characteristic (ROC) curve for the data presented in Fig. 7. The ROC curve shows the relationship of the threshold to the true and false positive rates for the binary classifier of an irradiated volume either having or lacking cancer cells. The ROC curve was generated by changing the threshold from 1σ to 3σ in 0.2σ increments and the results are plotted from right to left.

3.4 Detection from Centrifuged Blood

In the final part of this study, 1 mL of blood was centrifuged to remove erythrocytes and the remaining leukocytes were resuspended in 1 mL of $1\times$ PBS. About 300 μL of this solution was flowed through the system in order to parametrize the PA response of just leukocytes according to the two features used for classification. These parameters were then used for the automated identification of cancer cells, which produce PA signals with different features, among leukocytes. About 35 cancer cells were added to 1 mL of whole blood, the centrifugation procedure was used to remove erythrocytes, and
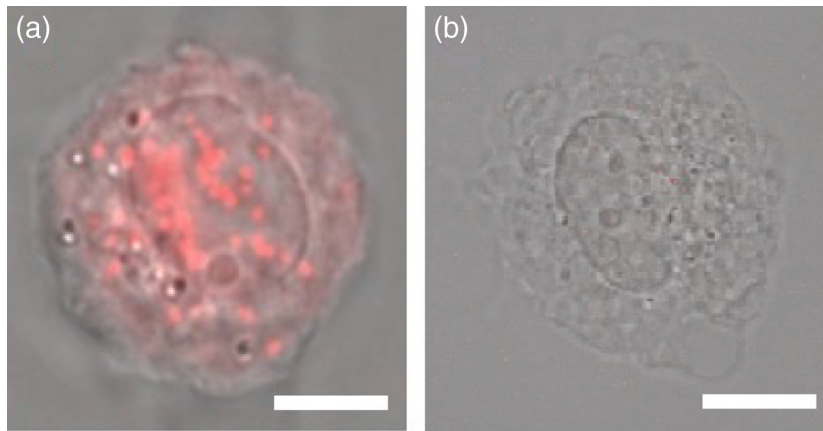
Fig. 5 Merged confocal fluorescence and transmission microscope image of two breast cancer cells. (a) A normal breast cancer cell with attached nanoparticles after exposure to anti-EpCAM labeled NPs. (b) An EpCAM receptor blocked cell with no attached nanoparticles after exposure to anti-EpCAM-labeled NPs. Scale bar is 5 μm.
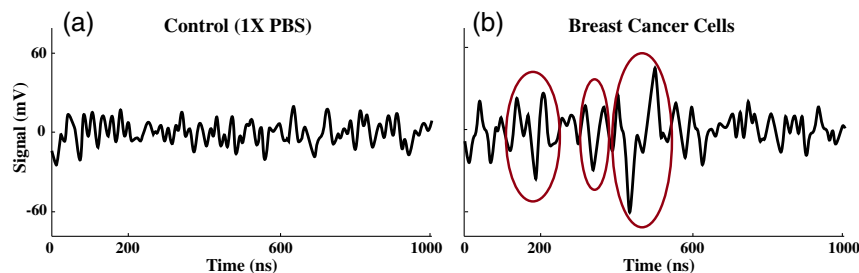

Fig. 6 (a) Plot of PA waveforms acquired during the PAFC test from laser irradiation of just 1× PBS and (b) with nanoparticle tagged breast cancer cells at a concentration of 670 cells/mL (2 cells/3 μL). The PAFC irradiates a 3-μL volume with every pulse, so we would expect an average of two cells in the chamber for every pulse. The three circles in part b designate three signals from three separate cells in the chamber.

the remaining leukocytes and cancer cells were resuspended in 1 mL of 1× PBS. The PAFC system was used to detect and capture the added cancer cells.

Figure 9 demonstrates the PA signals seen by the researchers during the flow tests. The trace in red is characteristic of when there are only leukocytes being irradiated and the blue trace

Fig. 7 A plot of each PA waveform in 2-D feature space from just 1× PBS (empty circles, black) and 1× PBS with nanoparticle tagged breast cancer cells (full circles, blue) at a concentration of 2 cells/3 μL.

shows the presence of a robust PA emitter between 850 and 900 ns. Even with cancer cells added, most PA signals resembled the red trace since the presence of a cancer cell in the chamber was an unlikely occurrence due to the small concentration.

This is especially supported by Fig. 10, which is a feature plot of every PA waveform acquired during the flow test for both samples. The waveforms from the initial sample of just leukocytes are plotted as squares ($n = 100$). The red dot at the center of the ellipse is the mean of that distribution and the ellipse is the 2.5σ boundary. The blue circles ($n = 400$) are all of the waveforms acquired during the PAFC test of the second sample, which was spiked with cancer cells. Most waveforms are within the red boundary and classified as not being different from just leukocytes. However, outside of the red boundary, toward the top-right, there are 17 outliers, which were classified by the automated system as containing cancer cells. These droplets were captured and imaged to find isolated cancer cells. The outliers at the bottom-left were not classified as containing cancer cells because their features were smaller than the mean and the voltage traces did not contain PA signals from cancer cells.

Figures 11(a) and 11(b) are light micrographs of 2 out of 15 total captured cancer cells, which were found in 13 of the 17 captured droplets. The remaining four droplets were not
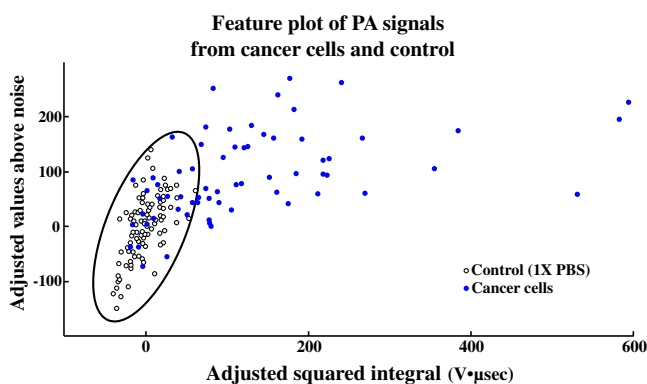
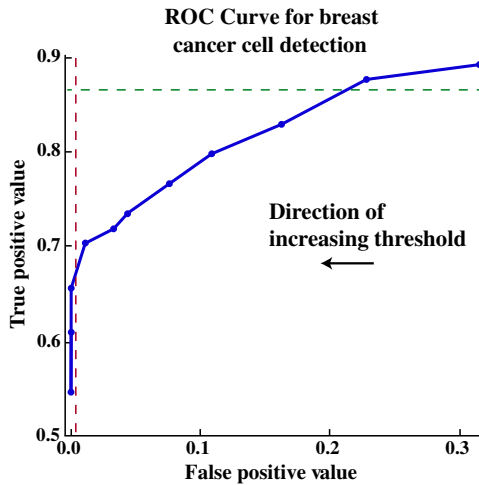## ROC Curve for breast cancer cell detection

Fig. 8 The ROC curve for binary classification of irradiated volumes as having or not having cancer cells. The green horizontal dashed line is the ideal true positive rate of 86.5% as explained within the text and the vertical dashed red line is the maximum acceptable false positive rate of 0.3% to reduce it to less than 1 per 1 mL of sample.
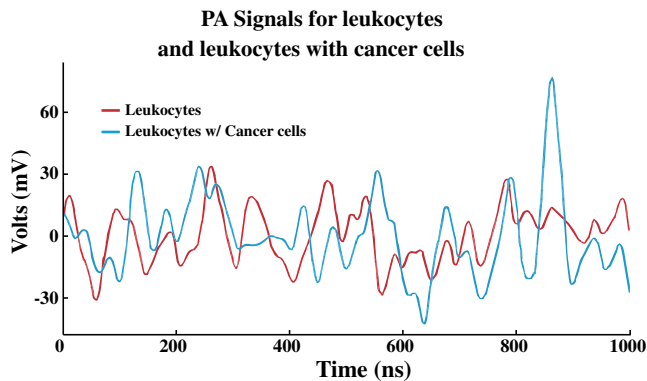
PA Signals for leukocytes and leukocytes with cancer cells

Fig. 9 (a) Plot of PA waveforms acquired during the PAFC test with detection of cancer cells from centrifuged blood. The red trace demonstrates the PA signal when there are no cancer cells but only leukocytes being irradiated in the chamber. The blue trace is the PA signal when there is a cancer cell among the leukocytes.
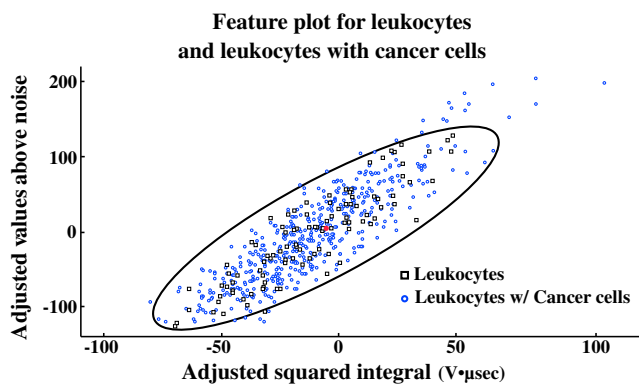
Feature plot for leukocytes and leukocytes with cancer cells

Fig. 10 A plot of each PA waveform in 2-D feature space from just leukocytes (square) and leukocytes with cancer cells (circle). About 35 cancer cells were added to 1 mL of blood and 17 points appear outside the boundary and are higher than the mean, which is marked by a full red dot. The outliers toward the bottom-left do not contain PA signals from cancer cells, as their features are much smaller than the mean.

found to contain cancer cells. Since the cancer cell nuclei were prelabeled with DAPI before they were added to the blood, researchers looked for cells with fluorescent blue nuclei. Out of the approximate 35 cancer cells added, 15 were successfully retrieved.

Finally, Fig. 12 demonstrates through a photo montage how a breast cancer cell can be captured and transported with a micromanipulator. Breast cancer cells were identified with DAPI fluorescence under microscopy and transported using a glass micropipette to a different dish with cytophilic wells, allowing for further immunohistochemical or genetic analyses.

4 Discussion

4.1 Nanoparticle Attachment and Specificity

The conjugation chemistry used to create the antibody-bound nanoparticles formed single groups of gold nanospheres attached to one fluorescent sphere, as well as large clusters of gold nanospheres attached to multiple fluorescent spheres, as evident in Fig. 2. These clusters may actually work to the benefit of the researchers as they provide large, concentrated doses of optical contrast to the cell. Moreover, from an acoustic standpoint, the 20-MHz transducer being used is unable to resolve and differentiate between ultrasound signals emitted from these larger clusters as opposed to single groups since they are both at or below 1 μm. Therefore, the presence of clusters should not change the detected frequency components of the PA signal.

The widefield microscopy used to generate the images for Fig. 3 is unable to optically resolve these 1 μm level clusters but it does demonstrate specificity of the nanoparticles to the cancer cells over leukocytes. However, there is nonspecific attachment of nanoparticles to leukocytes, as demonstrated by Fig. 3(b). About 5% to 10% of leukocytes are nonspecifically labeled with 10% to 17% of the average fluorescent intensity found on the average breast cancer cell. There are 10^6 to 10^7 leukocytes in 1 mL of human blood while there will be at most 10^3 cancer cells in 1 mL.[3,4] Even though they are not as photoacoustically active, this creates a significant number of background absorbers (about 200,000 to 500,000). Currently, blocking buffers composed of bovine serum albumin and mouse serum are being explored to reduce nonspecific labeling with promising results. Initially, blocking agents were not used in the labeling procedure in order to create the simplest possible technique. For these reasons of nonspecific labeling of leukocyte, cancer cells that were prelabeled with DAPI and nanoparticles were added to the vial of blood for the results presented in Sec. 3.4.

4.2 Detection and Classification of Breast Cancer Cells

The two features computed from the PA waveforms collected from each irradiation measure the presence of large variations from the mean. Both of these time-domain features are fairly intuitive since one is an integral and the other is a count of values above noise thresholds (positive and negative).

The method of classification being used with this feature set is threshold based since the distribution of features from the control of 1× PBS group parametrizes well to a bivariate normal distribution. Other parametric methods were difficult to pursue
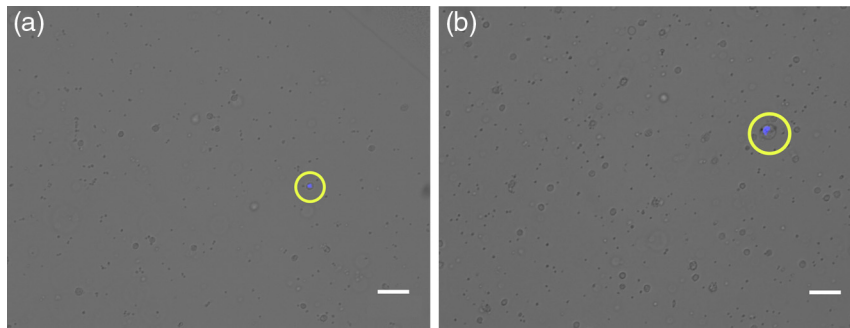
Fig. 11 Images of 2 out of 15 captured breast cancer cells (circled in yellow) that were retrieved through PAFC detection after ~35 cancer cells were added to 1 mL of whole blood. Cancer cells have DAPI-labeled nuclei, which are blue fluorescent.
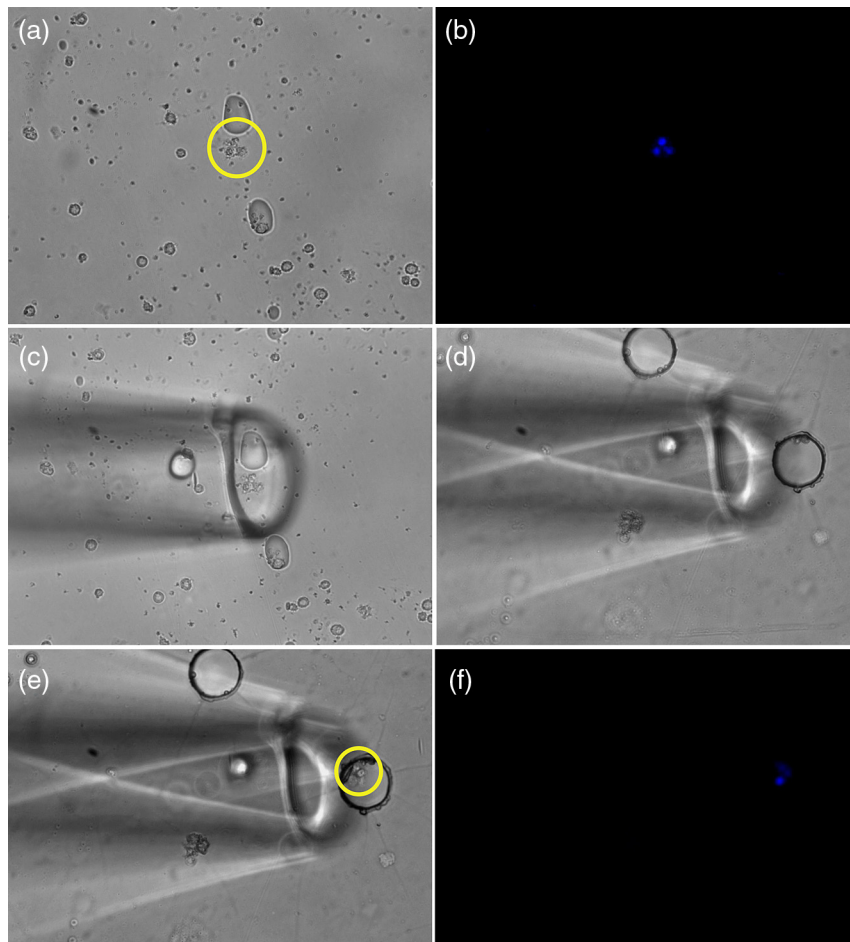

Fig. 12 How a breast cancer cell is captured out of solution and transported is demonstrated. (a) A small cluster of breast cancer cells is found (circled in yellow) and verified by visualizing DAPI labeling in (b). (c) A glass micropipette attached to a micromanipulator is used to remove the cell and transport it to a new dish shown in (c). This new dish has 100 μm cytophilic wells, which can hold the cells after they are placed within it as shown in (d). Finally, in (e), DAPI is again visualized to ensure that these are the same cells.

as the feature distribution from the breast cancer cell group was not easily described by mathematically tractable distributions.

It is important to note that though the expected value is 2 cells/3 μL, this will not be the case for every occurrence. Table 1 uses the Poisson distribution to calculate the probability of finding a specific number of cells in the irradiated volume of 3 μL given that the average rate is two cells. Since there will be 0 cells in the irradiated volume about 13.5% of the time, we should expect an ideal true positive rate of 86.5%, which has been marked with horizontal dashed green line in Fig. 8. However, to detect one cancer cell in 1 mL with certainty, the false positive rate must be reduced to below 1 per 1 mL of sample. Therefore, the maximum acceptable false positive rate must be <0.3% since the irradiated volume is 3 μL. The

Table 1 Expected value of two cells.

Number of cells	Probability
0	0.135
1	0.271
2	0.271
3	0.180
4	0.090
5	0.036
6	0.012
7	0.003

red vertical dashed line in Fig. 8 marks this maximum acceptable false positive rate, which is paired with an approximate true positive rate of 67% with a threshold larger than 2.4σ. Moreover, the slope of the ROC curve changes from greater than 1 to less than 1 at the threshold of 2.4σ, implying that for every incremental increase in the false positive rate, there is a smaller increase in the true positive rate. This demonstrates that there are diminishing returns when the threshold is reduced beyond 2.4σ.

According to the Poisson distribution, the probability of finding two or more cells in the irradiated volume is 0.592 and a larger proportion of 0.67 is classified as true positive, implying a detection limit between one and two cells for the flow system. This is understandable since Bhattacharyya et al.[12] have shown that the nanoparticle load from one cancer cell to another can vary.[12] Moreover, the position of the cell in the beam spot can also change the sensitivity of the system as the energy profile and acoustic sensitivity are not uniform across the irradiated area or volume.

4.3 Detection and Retrieval of Cancer Cells from Blood

About 35 cancer cells were added to 1 mL of blood and 15 were isolated, located, and imaged. However, the initial number of cancer cells added to blood was probably not exactly 35, since a small volume of stock breast cancer cell suspension was added to the blood. It is safer to assume that the initial number of cancer cells added was within 25 to 45 cells if the variance is assumed to be equal to the expected value when drawing from a large sample.

Moreover, the centrifugation procedure used to remove erythrocytes causes 10% to 30% cell loss for leukocytes and cancer cells.[18] This implies that the total number of cancer cells had been reduced to 17 to 40 cells even before the solution was tested with the PAFC. The automated system classified 17 signals as being different from leukocytes but only 15 cells were found in 13 of the droplets. This may be because some cells were lost due to the inefficiency of the capturing protocol. For this study, droplets were captured manually but this procedure is being automated to provide more consistent results. When the system detected a cancer cell, the droplet was captured downstream of where it was irradiated after a specific amount of

time, which allowed the droplet to reach the end of the chamber. It is also possible that the remaining four droplets never contained any cancer cells and were false positives. This is slightly higher than the expected number of false positives (<1), which could be caused by stray erythrocytes.

Since 15 cells were captured and about 35 cells were added, the retrieval rate of the entire protocol with the *in vitro* PAFC is ~43%. Nonetheless, it is difficult to determine an exact retrieval rate since there could have been as few as 25 cancer cells added to the blood. If the retrieval rate is indeed 43%, at least four cancer cells would have to be present in 1 mL of blood to have about a 90% chance of retrieving one cell. Though Giuliano et al.[4] have found with the CellSearch system that 5 cancer cells/7.5 mL of blood has significant prognostic value, Kirby et al.[5] have argued with the geometrically enhanced differential immunocapture system that CellSearch underestimates the cancer cell concentrations by 2 to 400 times. From these sources it can be inferred that the *in vitro* PAFC system detects clinically relevant concentrations of cancer cells in blood.

The advantages of this technology over existing CTC technologies is that the cells remain in suspension and are never attached to a substrate like many antibody technologies. Additionally, it does not depend on size or mechanical stiffness like many technologies, as these parameters have a huge biological variability.

However, it is important to remember that the cancer cells had been prelabeled with both DAPI and nanoparticles before they were added to the blood. In a clinical blood test, the cancer cells in the blood cannot be prelabeled but must be specifically labeled in the presence of leukocytes. As mentioned in Sec. 4.2, the antibody mediated labeling procedure is currently being developed since there is some nonspecific labeling of leukocytes with nanoparticles. However, once nonspecific labeling is reduced, similar retrieval rates are expected since the PAFC is able to detect the presence of one to two cancer cells in the chamber.

Figure 11 shows images of two different captured cancer cells surrounded by leukocytes. The red fluorescence from the fluorescent-gold particle was bleached when the cells were irradiated with the PAFC, making DAPI the only characteristic stain on the cancer cells. Though this method of identification was adequate for this study, a different method of identifying cancer cells will have to be used for a clinically relevant test. The captured breast cancer cells could be labeled with fluorescent antibodies for human epidermal growth factor receptor 2 or human milk fat globulin for secondary verification and visual identification, as these are known to be overexpressed in breast cancers.[19,20]

Finally, Fig. 12 demonstrates how the identified cell could then be removed from the solution with a micromanipulator controlled micropippette and transported to another location. In this case, the cells are transported to a 100-μm cytophilic well in a different slide. However, this new location can be the cap of a polymerase chain reaction (PCR) tube filled with cell lysis buffer to start the first step to an quantitative reverse transcription PCR method or it could be a Petri dish filled with culture media in order to culture this captured cancer cell.

This technique can be modified to apply to other cancers by changing the antibody conjugated to the nanoparticles used for PA contrast. This study demonstrates the ability to capture single circulating cells and is a path toward the possibilities that are sure to transform oncology in the next few decades.

References

1. I. R. Hart and I. J. Fidler, "Role of organ selectivity in the determination of metastatic patterns of B16 melanoma," *Cancer Res.* **40**, 2281–2287 (1980).
2. P. Paterlini-Berchot and N. L. Benali, "Circulating tumor cells (CTC) detection: clinical impact and future directions," *Cancer Lett.* **253**, 180–204 (2007).
3. M. C. Miller, G. V. Doyle, and L. W. M. M. Terstappen, "Significance of circulating tumor cells detected by the CellSearch system in patients with metastatic breast colorectal and prostate cancer," *J. Oncol.* **2010**, 617421 (2010).
4. M. Giuliano et al., "Circulating tumor cells as prognostic and predictive markers in metastatic breast cancer patients receiving first-line systemic treatment," *Breast Cancer Res.* **13**, R67 (2011).
5. B. J. Kirby et al., "Functional characterization of circulating tumor cells with a prostate-cancer-specific microfluidic device," *PLoS One* **7**, e35976 (2012).
6. E. Galanzha et al., "In vivo, noninvasive, label-free detection and eradication of circulating metastatic melanoma cells using two-color photoacoustic flow cytometry with a diode laser," *Cancer Res.* **69**, 7926–7934 (2009).
7. G. Gutierrez-Juarez et al., "Detection of melanoma cells in vitro using an optical detector of photoacoustic waves," *Lasers Surg. Med.* **42**, 274–281 (2010).
8. J. Viator et al., "Gold nanoparticle mediated detection of prostate cancer cells using photoacoustic flowmetry with optical reflectance," *J. Biomed. Nanotechnol.* **6**, 187–191 (2010).
9. E. Galanzha et al., "In vivo magnetic enrichment and multiplex photoacoustic detection of circulating tumour cells," *Nat. Nanotechnol.* **4**, 855–860 (2009).
10. D. McCormack et al., "Enhanced photoacoustic detection of melanoma cells using gold nanoparticles," *Lasers Surg. Med.* **43**, 333–338 (2011).
11. D. Nedosekin et al., "In vivo ultra-fast photoacoustic flow cytometry of circulating human melanoma cells using near-infrared high-pulse rate lasers," *Cytometry* **79A**, 825–833 (2011).
12. K. Bhattacharyya et al., "Gold nanoparticle-mediated detection of circulating cancer cells," *Phys. Med. Biol.* **60**, 3081–3096 (2015).
13. K. Bhattacharyya et al., "Gold nanoparticle-mediated detection of circulating cancer cells," *Clin. Lab. Med.* **32**, 89–101 (2012).
14. E. I. Galanzha and V. P. Zharov, "Circulating tumor cell detection and capture by photoacoustic flow cytometry in vivo and ex vivo," *Cancers* **5**, 1691–1738 (2013).
15. C. O'Brien et al., "Capture of circulating tumor cells using photoacoustic flowmetry and two phase flow," *J. Biomed. Opt.* **17**, 061221 (2012).
16. S. Gupta et al., "Photoacoustic detection of induced melanoma in vitro using a mouse model," *Proc. SPIE* **8214**, 821414 (2012).
17. M. Ishii, "Thermo-fluid dynamic theory of two-phase flow," in *NASA STI/Recon Technical Report A*, Vol. **75**, p. 29657, NASA Scientific and Technical Information Program, Hampton, Virginia (1975).
18. R. Gertler et al., "Detection of circulating tumor cells in blood using an optimized density gradient centrifugation," *Recent Results Cancer Res.* **162**, 149–155 (2003).
19. J. Baselga et al., "HER2 overexpression and paclitaxel sensitivity in breast cancer: therapeutic implications," *Oncology* **11**, 43–48 (1997).
20. J. Burchell et al., "Development and characterization of breast cancer reactive monoclonal antibodies directed to the core protein of the human milk mucin," *Cancer Res.* **47**, 5476–5782 (1987).

Kiran Bhattacharyya is a doctoral candidate at Northwestern University in the Biomedical Engineering Department. He received his BS and MS degrees in bioengineering from the University of Missouri. His research interests include applying biomedical optics and nanotechnology methods to cancer detection, cellular analysis and manipulation, and neuroscience.

Benjamin S. Goldschmidt is an assistant professor of biomedical engineering at Duquesne University. He received his BS and PhD degrees in bioengineering from the University of Missouri in Columbia, where he worked on photoacoustic flow cytometry and developed total internal reflection methods using photoacoustics. He is actively involved in biomedical optics, particularly in the areas of photoacoustics and materials characterization. He also has experience in commercialization of optical technologies for human health.

John A. Viator is a professor and founding director of the Biomedical Engineering Program at Duquesne University. He is also an adjunct professor of bioengineering at the University of Pittsburgh. He received his PhD in electrical engineering from Oregon Health & Science University. He has held positions at the University of California, Irvine, and the University of Missouri prior to arriving at Duquesne. His research interests are in biomedical optics, specifically in photoacoustic sensing and imaging.